Reliability Benchmarking Novel Ag-sinter Die-Attach Against High-Pb Solder Under Thermal Cycling and High-Temperature Storage Testing

Henry A. Martin[1,2], B. Senthil Kumar[3],
Frans G. M. Meeuwsen[1,2], Edsger C. P. Smits[1,2], Ruud D. Wit[1,2],
Liu Yu[3], Tan Tze Qing[3].

[1]Netherlands Organisation for Applied Scientific Research (TNO), Den Haag, The Netherlands.
[2]Chip Integration Technology Center (CITC), Nijmegen, The Netherlands.
[3]Heraeus Materials Singapore Pte. Ltd., Pioneer Crescent, Singapore.

henry.martin@tno.nl ; senthilkumar.balasubramanian@heraeus.com

Abstract

Continued reliance on high-Pb solders for die-attach applications in discrete power semiconductor packaging remains a major challenge in achieving fully Pb-free manufacturing. Although pressureless Ag-sintering emerged as a promising alternative, demonstrating its suitability as a drop-in replacement requires compatibility with high-volume manufacturing processes. In this study, a practical set of processability and reliability requirements was established to evaluate a pressureless pure Ag-sinter material (DA252) formulated by Heraeus as a Pb-free alternative. The DA252 material was assessed on automotive-grade PQFN-packaged Si-MOSFETs and benchmarked against standard high-Pb (Pb92.5Sn5Ag2.5) solder. Processability was assessed through bondline thickness, void content, and die-shear strength, while reliability was investigated through thermal cycling ($-55°C$ to $150°C$ for 2000 cycles) and high-temperature storage ($150°C$ for 2000 hours) tests. Device health was monitored through changes in on-state resistance ($R_{DS(on)}$), following AEC-Q101 qualification criteria. The evaluated pressureless Ag-sinter paste exhibited a homogeneous die-attach interface with bondline shrinkage below 25%, average void content below 0.2%, and a die shear strength > $1.5 Kg/mm^2$ (>15MPa) at both RT & $260°C$. During thermal cycling, the Ag-sintered samples maintained a relatively stable electrical performance compared to the benchmarked high-Pb solder, particularly for larger die configurations where thermomechanical stresses were most severe. Stable electrical characteristics were also observed over 2000 hours of high-temperature storage testing. The results presented in this study demonstrate the processability and reliability of pressureless cured pure Ag-sinter DA252 material in cost-sensitive high-volume discrete power semiconductor packaging. Complementary failure analysis and inspection on microstructural evolution are further required to warrant the DA252 material's robustness.

Key words

Discrete power semiconductors; Pb-solder replacement; Pressureless Ag-sintering.

I. Introduction

The 2025 Nobel Prize in Economic Sciences was awarded for the theory of sustained economic growth through "creative destruction" – the principle that true industrial leaps require deliberate dismantling of legacy paradigms [1]. For decades, the power semiconductor industry has operated under a persistent paradigm, relying on RoHS regulatory exemptions to utilize high-Pb solders for die-attach applications. While chip architectures in discrete power semiconductors have leaped forward, a drop-in replacement for high-Pb solders that satisfies high-throughput package assembly requirements and that meets automotive reliability qualification standards (AEC Q100 & Q101) is yet to materialize.

Several Pb-free alternative bonding mechanisms have been evaluated over the years, namely eutectic bonding, transient liquid-phase bonding (TLPB), and solid-state bonding. However, each bonding mechanism presents a distinct trade-off between its processing window and operational stability. For instance, high-temperature eutectics (e.g., Au-Si or Au-Ge), though favorable for improved thermal performance, hermeticity, and no outgassing, still suffer from severe thermomechanical stresses due to high processing temperatures ($\sim 360°C$) and mismatched thermal expansion coefficients [2, 3]. Conversely, low-temperature eutectics (e.g., Au-Sn) are processed at $\sim 280°C$, which induces lower residual stresses, yet suffer from brittle failures due to high elastic modulus [4, 5]. Meanwhile, TLPB remains heavily bottlenecked by longer processing time that challenges high-throughput operations and severe micro-voiding along the intermetallic interfaces [6, 7]. In contrast, sintering technology circumvents the drawbacks inherent to liquid-phase methods in eutectic and TLPB by operating through solid-state diffusion.

Sintering involves fusion of metallic particles under heat and, optionally, under pressure. A primary differentiator of sintering is the ability to process materials at relatively low temperatures, typically between 200 and 300°C, while yielding an interface with the high melting point characteristics of a bulk metal. This unique capability led to the adoption of sintering for power modules by Semikron in 2007, where IGBT devices were pressure-sintered using Ag-particles onto DBC substrates at temperatures $< 250°C$. The sintered joints exhibited a homogeneous interface with superior electrical, thermal, and mechanical performance compared to high-Pb solders [8].

While pressure-assisted sintering has since achieved widespread adoption in power modules, its application in high-volume, cost-sensitive discrete power semiconductors remains heavily constrained. This commercial bottleneck is primarily due to the risk of die cracking when uniform pressure is applied to non-planar discrete leadframes, as well as the capital expenses associated with modifying established, high-throughput legacy reflow manufacturing lines. Hence, based on past experiences, CITC (part of TNO) defined the following set of requirements for assessing sintering materials as a drop-in replacement for high-Pb solders in discrete power semiconductors:

- **Storage and homogeneity:** The paste must exhibit high resistance to phase separation and sedimentation during transport and storage (RT / $-20°C$ / $-40°C$), while remaining readily dispensable or printable, with centrifugal mixing required only as an optional pre-processing step.

- **Rheology and substrate compatibility:** The paste rheology must remain stable post-dispensing or printing, and it can directly adhere onto surface-cleaned bare-copper leadframes.

- **Staging time stability:** The dispensed or printed paste chemistry must remain stable over open-face staging time – the time between applying paste and die-bonding, without altering the material's wetting dynamics.

- **Curing conditions:** The paste must be cured pressureless within a standard industrial convection box oven under the following atmospheric options - Ambient air / Nitrogen (N_2) / Forming gas ($5\%H_2N_2$), with permissible O_2 level $\sim$100 – 1000PPM.

- **Post cure conditions:** The solvents or binders in the paste must cleanly volatilize during sintering without leaving organic residues with less than 1% voiding. The post-sintered surface must be pristine, and any remaining residues must be removable by a standard plasma cleaning protocol before wire bonding and molding.

- **Reliability criteria:** The AEC-Q101 standard for discrete semiconductors mandates that the electrical parameters, namely on-state electrical resistance ($R_{DS(on)}$) or Threshold Voltage ($V_{GS(th)}$) for MOSFETs must not shift by more than ±20% of their initial (pre-stress) value over 1000 thermal cycles from $-55°C$ to $150°C$.

In this study, a pressureless pure Ag-sinter material (DA252) formulated by Heraeus was evaluated based on the above-mentioned criterion. This paper presents experimental validation of the proposed paste by investigating its processability for package assembly and its lifetime performance. The performance is benchmarked against standard high-Pb solder (PbSn5Ag2.5) on a PQFN package platform with bare-copper Leadframe and two different Si-MOSFET die sizes. The processing parameters investigated in this study include bond-line thickness measurements (wet and post-cured), voiding % inspected through X-ray imaging, and cold (RT) and hot (260°C) die-shear strength. Subsequently, the lifetime performance was evaluated by subjecting the packaged devices to thermal cycling and high-temperature storage testing. The MOSFET's on-state electrical resistance $R_{DS(on)}$ parameter was monitored intermittently as a health indicator of the device performance and the die-attach interface stability.

The remainder of this paper is organized as follows: Section II details the experimental methodology, which includes sample preparation (Section II-A), preliminary inspection (Section II-B), and the conditions for accelerated lifetime tests (Section II-C). Section III presents the lifetime reliability test results by systematically analyzing the $R_{DS(on)}$ parameter of devices under thermal cycling (Section III-A) and high-temperature storage conditions (Section III-B). A detailed discussion is provided in Section IV, with a brief conclusion in Section V.

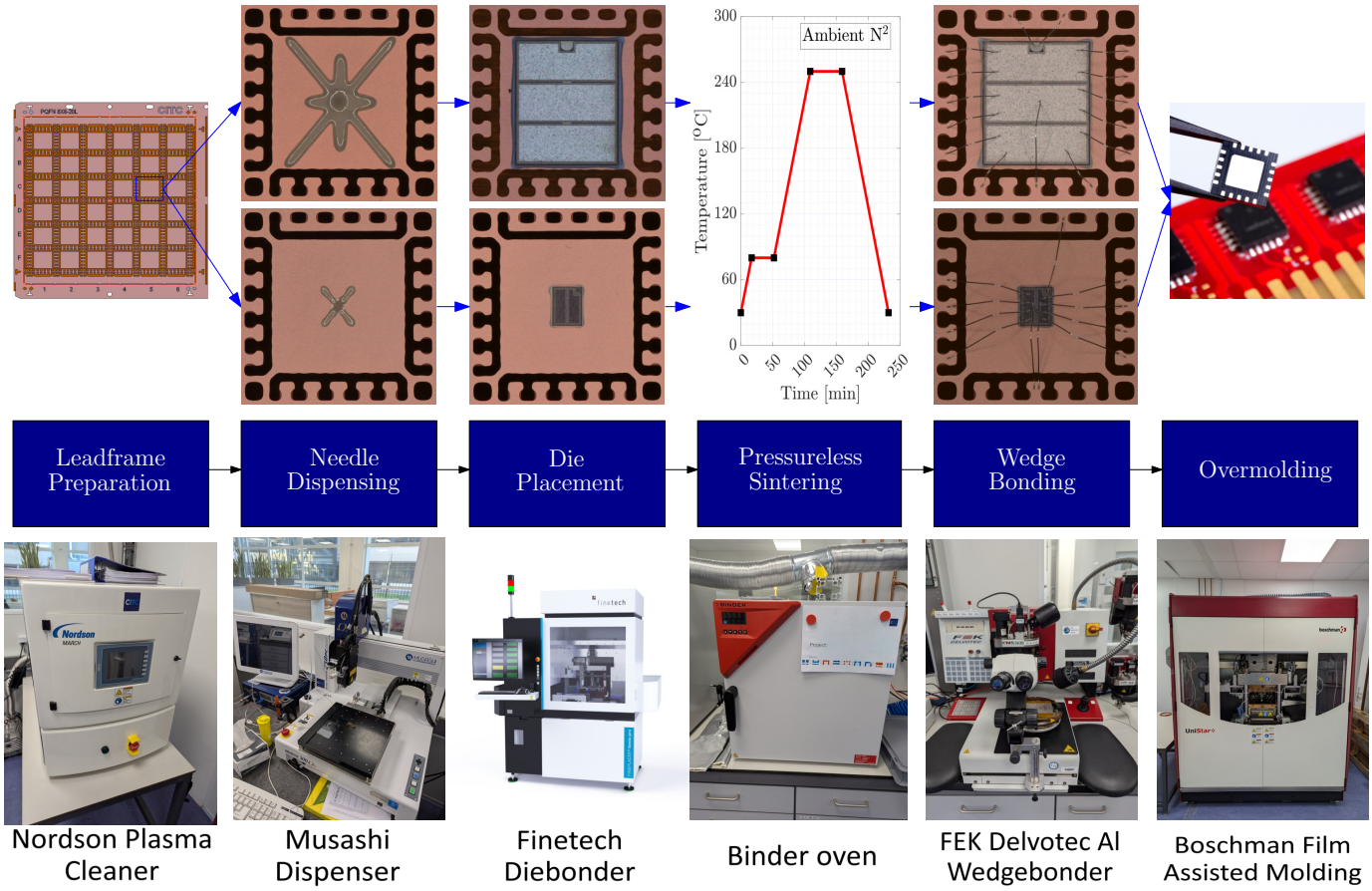


Figure 1: Assembly Overview

II. Experimental Methods

A. *Sample Preparation*

The test vehicles used in this study are Silicon-based N-channel enhancement mode field-effect transistors (MOSFETs) that are commercially used in high-performance automotive systems. Two different die sizes were evaluated:

- **Type 1 (Large Die):** 4.5mm × 5.5mm × 175μm with AlCu top-side metallization and TiNiAg back-side metallization.
- **Type 2 (Small Die):** 1.2mm × 1.6mm × 150μm with AlCu top-side metallization and TiNiAg back-side metallization.

Both die types were packaged in a Power Quad Flat No-Lead (PQFN) wire-bonded surface-mount platform, and the assembly steps are explained as follows;

1. The leadframe used is a C194 fully hardened bare copper 500μm thick leadframe that is treated with a standard reflow profile of 260°C peak under N_2 ambient for Organic Surface Protection (OSP) removal, and subsequently treated with Argon plasma to remove surface contamination.
2. DA252 is a dispensable paste that was stored at −20°C and was acclimatized to ambient conditions for two hours before dispensing. The paste was dispensed in a snowflake pattern using a Musashi dispenser with a 22-gauge needle of 0.41mm in diameter at a pressure of ∼ 70 – 160KPa. Two different patterns were dispensed, and each pattern was optimized according to the die size.
3. Upon dispensing, both die types were placed within a staging time of 15 minutes using a Finetech position-controlled die-bonder for achieving a uniform wet paste bondline thickness (∼40μm for large dies and ∼30μm for small dies) and a target fillet height of ∼50% of die thickness. Subsequently, both die types were cured in a binder oven at an initial drying temperature of 80°C and a final sintering temperature of 250°C. The curing was completely done under N_2 ambient with an O_2 level maintained below 300 ppm.
4. Subsequently, the assembled die and leadframe surfaces were cleaned using Argon plasma to remove surface contamination while curing. The die top surfaces were further wedge-bonded using 50μm AlSi1%. A 4-point electri-

cal configuration was set up between the source (die top surface) and the drain terminals (leadframe bottom contact) for precise electrical resistance measurements that include the die-attach interface. The samples were further overmolded with Sumitomo EME-G700LA epoxy molding compound at 175°C and subsequently laser marked for identification and singulated.

5. All singulated packages underwent Moisture Sensitivity Level 3 (MSL3) pre-conditioning, which involves drying at 125°C for 24 hours, followed by soaking at 60% relative humidity at 60°C for 42 hours, and subjecting the samples to three consecutive reflow cycles at 260°C, with the third cycle being the reflow soldering of packages onto PCBs.

For the baseline comparison, identical packages were assembled using a standard high-Pb solder paste (Pb92.5Sn5Ag2.5). These reference samples required stencil printing instead of dispensing, force-controlled die-placement instead of position-controlled, and were reflowed at 360°C in a vacuum environment. Before mounting onto the PCB, all sample groups (both Ag-sinter and high-Pb solder) were visually inspected. Any samples displaying physical inconsistencies, such as excessive die tilt, insufficient paste coverage below the die, inadequate die-fillet height, or flaws in wedge bonds, were discarded. An overview of defect-free samples that are soldered onto PCBs for further lifetime testing is shown in Table 1.

Table 1: Experimental Matrix

Die Size	Die-Attach	Total Samples
Large Die ($4.5 \times 5.5\,\text{mm}^2$)	Pb92.5Sn5Ag2.5	18
	DA252	66
Small Die ($1.2 \times 1.6\,\text{mm}^2$)	Pb92.5Sn5Ag2.5	45
	DA252	57

B. *Preliminary Inspection*

Preliminary inspection of DA252 paste was performed to evaluate the integrity of the die-attach interface post-curing. Using a position-controlled die-bonder, a uniform wet paste bondline thickness (BLT) was maintained (~40μm for large dies and ~30μm for small dies). Upon curing, the final BLT was determined to be between ~30 – 35μm for large dies and ~25μm for small dies. This indicates a volumetric shrinkage of less than 25% during the solid-state densification process. Subsequently, the samples were inspected non-destructively using X-ray imaging to analyze the die-attach interface. Across all inspected samples, the average void fraction remained below 0.2% of the total die area, confirming a homogeneous interface without void entrapments (see Figure 2). The average BLT (both wet and cured) and the average void % values are reported in Table 2. It should be noted that these averages only represent the defect-free DA252 samples mentioned in Table 1, as samples rejected due to physical inconsistencies were excluded.

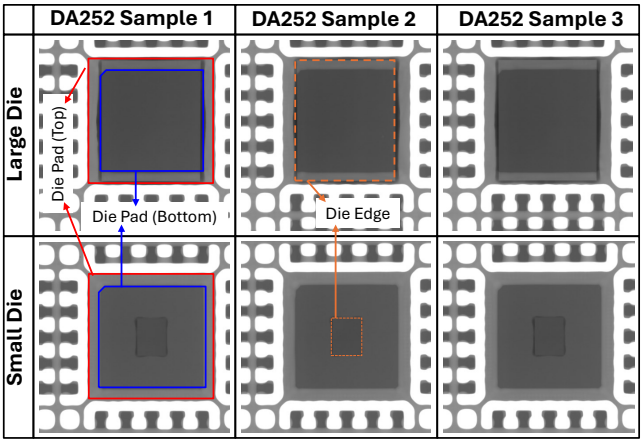


Figure 2: X-ray inspection images of DA252 samples indicating no signs of voiding.

Table 2: Die-attach interface characteristics

Parameter	DA252	
	Large Die	Small Die
Avg. BLT (wet)	~40 μm	~30 μm
Avg. BLT (cured)	~30 – 35 μm	~25 μm
Avg. Void %	$< 0.2\%$	$< 0.2\%$
Avg. CDSS	~17 MPa	~20 MPa
Avg. HDSS	~24 MPa	~33 MPa

To further assess the mechanical robustness of the post-cured die-attach interface, specialized test vehicles that followed the identical processes outlined in Figure 1 were prepared on bare copper coupons. These coupons are suitable for die-shear testing at room temperature (Cold Die Shear Strength CDSS) and at 260°C (Hot Die Shear Strength HDSS). The smaller dies exhibit higher shear resistances than the larger dies at room temperature and at 260°C. Notably, the DA252 paste exhibits higher shear strength at 260°C than at room temperature. Initially, this was suspected to be an artifact of insufficient curing, as the hot-die shear tests at 260°C exceeded the maximum curing temperature of 250°C. However, it is hypothesized that this increase is more likely driven by the high-temperature relaxation behavior of the

material, which requires further investigation. The CDSS and HDSS values are reported in Table 2, which is an average of five samples per type.

C. Lifetime Testing Conditions

To systematically evaluate the long-term reliability of the die-attach interfaces, the packages (see Table 1) were subjected to two different accelerated lifetime testing protocols, the thermal cycling test and high-temperature storage test, as summarized in Figure 3. Thermal cycling tests are targeted to characterize the thermomechanical fatigue resistance, driven primarily due to the mismatch in thermal expansion coefficient (CTE) between the silicon die and the copper leadframe. The samples were subjected to cyclic temperature swings from $-55°C$ to $150°C$ with a dwell time of 10 minutes at extreme temperatures. The tests were carried out for an extended duration of 2000 thermal cycles, which is twice the thermal cycling requirement specified in AEC-Q101. To monitor the package performance degradation, intermediate electrical measurements of all samples were conducted at predefined read points: 0 (post-MSL3), 100, 200, 500, 1000, 1500, and 2000 thermal cycles. The AEC-Q101 qualification criterion specifies less than 20% shift in on-state resistance ($\Delta R_{DS(on)}$) over 1000 cycles. In parallel, high-temperature storage tests were conducted to analyze the stability of the die-attach interface over 2000 hours of storage at extreme high temperature $150°C$. Electrical measurements were performed intermittently at 0, 500, 1000, and 2000 hours. Consistent with the thermal cycling protocol, the failure threshold was defined as a $\Delta R_{DS(on)}$ shift exceeding 20%.

Given that the severity of thermal cycling is higher than that of high-temperature storage testing, the benchmarking of Ag-sinter paste against standard high-Pb solder was evaluated solely with thermal cycling. Consequently, all Pb92.5Sn5Ag2.5 reference samples specified in Table 1 were used for thermal cycling tests and, the DA252 samples specified in Table 1 were split across both tests to provide comprehensive evidence on thermo-mechanical fatigue resistance and demonstrate the stability of the material over extended operation at high temperatures.

III. Experimental Results

To evaluate the performance of the die-attach interface during thermal cycling and high temperature storage testing, the dynamic on-state resistance ($R_{DS(on)}$) was chosen as the primary performance metric. The $R_{DS(on)}$ is measured across the drain-source terminals under forward bias (V_{GS} = 10V & I_D = 1A), and it represents the cumulative electrical resistance of the silicon die, the die-attach interface, and the copper leadframe. Hence, degradation within the die-attach interface, such as thermo-mechanical fatigue or delamination, would directly impede the current path, resulting in a measurable increase in the $R_{DS(on)}$. The measurement results are presented in figures 4 (TCT) and 5 (HTS test). The 0-cycle and 0-hour $R_{DS(on)}$ measurements highlight the following differences across the sample groups:

- Firstly, packages with high-Pb solder have a relatively higher mean $R_{DS(on)}$ than the Ag-sinter material. These differences are due to the intrinsic material properties, i.e, the DA252 Ag-sinter has $\sim 20\times$ lower electrical resistivity than Pb92.5Sn5Ag2.5 solder.
- Secondly, packages with smaller dies exhibit higher $R_{DS(on)}$ than larger dies. Since the internal resistive components of a MOSFET are inversely proportional to its active channel area, the smaller dies inherently have a higher $R_{DS(on)}$ compared to the larger dies.

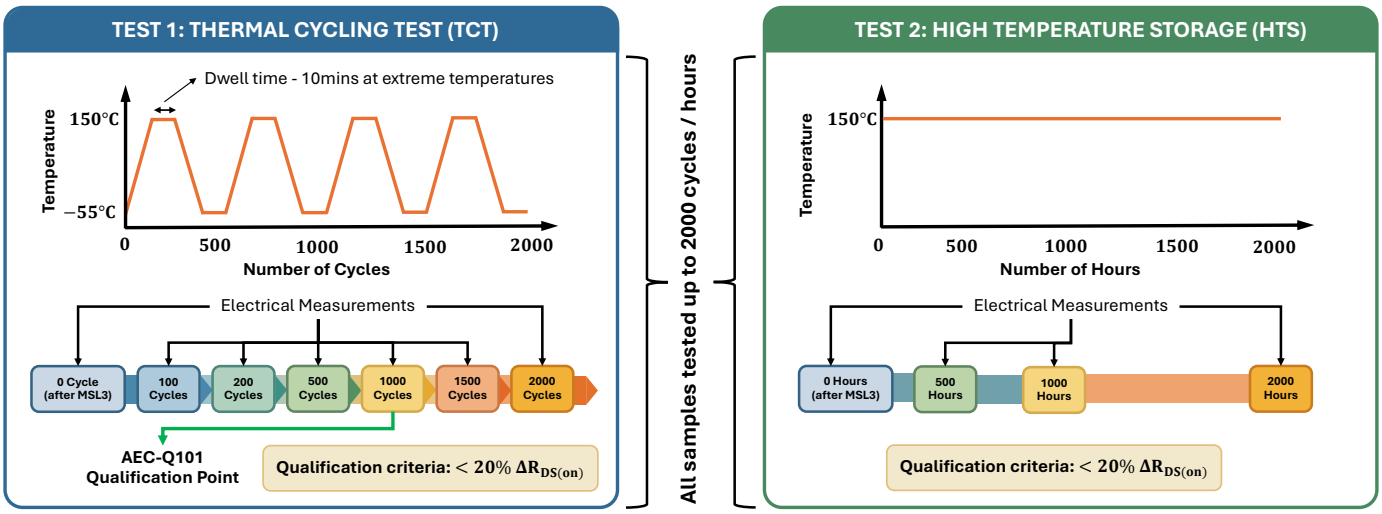
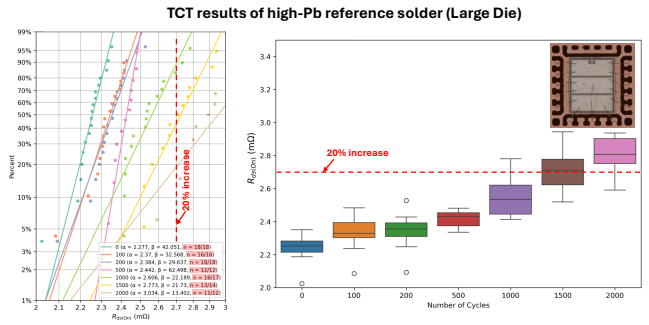
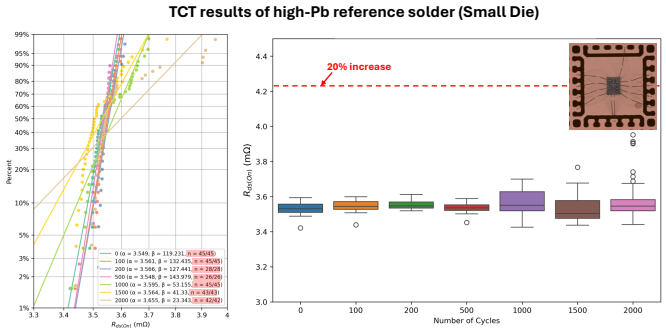


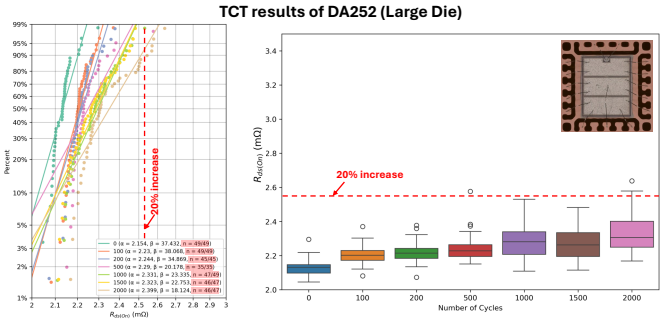
Figure 3: Overview of accelerated lifetime testing conditions, measurement protocols, and qualification criteria.



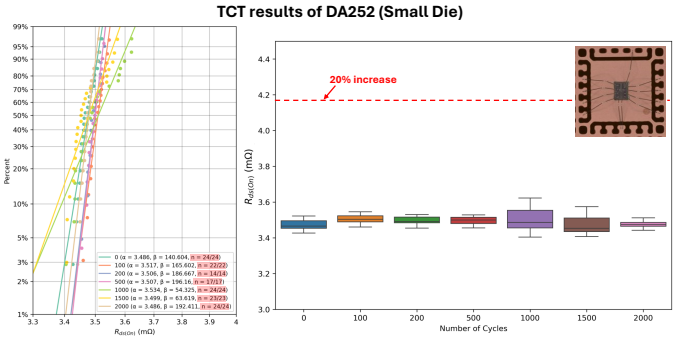
(a) Weibull and box plots of high-Pb reference solder with a Large die



(b) Weibull and box plots of high-Pb reference solder with a Small die



(c) Weibull and box plots of DA252-A material with a Large die



(d) Weibull and box plots of DA252-A material with a Small die

Figure 4: Thermal cycling test results for DA252 Ag-sinter benchmarked against Pb92.5Sn5Ag2.5 over 2000 cycles from −55°C to 150°C, represented via probability distribution and interquartile range (IQR) box plots of dynamic on-state resistance ($R_{DS(on)}$). α represents the scale parameter, which is the characteristic value ($R_{DS(on)}$), and β represents the shape parameter, which is the slope of the fitted line. 'n' highlighted in red denotes the sample quantity per read point. A decrease or increase in 'n' is due to measurement issues. The dashed red line indicates the relative 20% failure threshold.

To make an equitable comparison across both material types and die sizes, the 20% threshold is chosen relative to the 0-cycle mean $R_{DS(on)}$ of each specific sample type. The changes in $R_{DS(on)}$ over the testing duration are visually presented as Weibull probability distributions and interquartile range (IQR) box plots in figures 4 & 5. A linear relationship is fitted to the probability distributions at every read point. The degradation behavior can be directly inferred based on the changes in the fitted line.

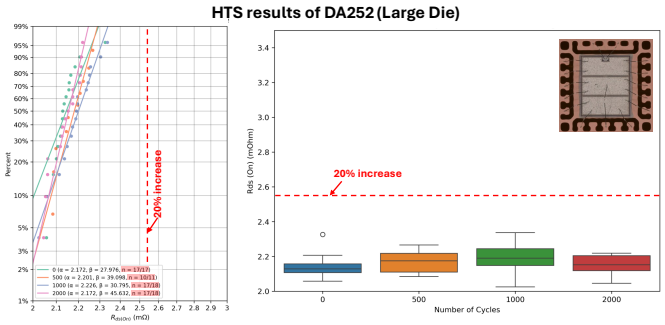
In figures 4 & 5, the probability distribution plots contains α and β parameters. Here, α represents the scale parameter, which is a characteristic mean $R_{DS(on)}$ at which the sample population lies along the horizontal axis, while β represents the shape parameter, corresponding directly to the slope of the fitted linear regression line. A decreasing β value over the testing duration indicates a broadening variance and non-uniform degradation within the sample group. Complementing the probability distribution are the corresponding box plots that provide a simple visual indication of the device performance.

A. *Thermal Cycling Tests (TCT)*

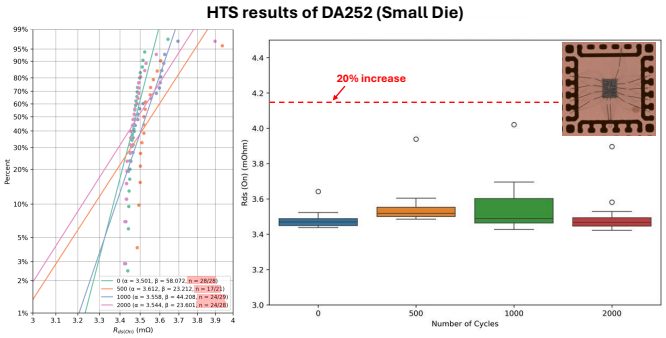
Under thermal cycling test conditions, the most severe thermo-mechanical stresses were observed on samples with large dies due to the CTE mismatch across a larger footprint area.

- In figure 4a, the reference high-Pb solder samples indicate a systematic increase in $R_{DS(on)}$ over 2000 thermal cycles. The upper statistical limit of the high-Pb samples breached the 20% failure threshold at the 1000-cycle read-point, and the mean $R_{DS(on)}$ clearly exceeded the failure criterion by the 2000-cycle end-of-life point. Besides, figure 4a shows higher variance in the probability distribution of high-Pb solders over time, thereby indicating non-uniform degradation across the sample population.
- In contrast, the large dies assembled with Ag-sinter material maintained relatively stable $R_{DS(on)}$ (figure 4c), while some outlier samples exceeded the threshold. Notably, Ag-sinter has lower variance in its probability distribution, signifying uniform degradation.

The smaller footprint area proportionally reduced the ther-



(a) Weibull and box plots of DA252 material with a Large die.



(b) Weibull and box plots of DA252 material with a Small die.

Figure 5: High-Temperature Storage (HTS) test results for DA252 Ag-sinter paste over 2000 hours at 150°C, represented via probability distribution and interquartile range (IQR) box plots of dynamic on-state resistance ($R_{DS(on)}$). α represents the scale parameter, which is the characteristic value ($R_{DS(on)}$), and β represents the shape parameter, which is the slope of the fitted line. 'n' highlighted in red denotes the sample quantity per read point. A decrease or increase in 'n' is due to measurement issues. The dashed red line indicates the relative 20% failure threshold.

momechanical stresses on the small die compared to the large die configurations. Consequently, the high-Pb solder samples (see Figure 4b) and the Ag-sinter samples (see Figure 4d) maintained mean $R_{DS(on)}$ values well within the 20% threshold even after 2000 thermal cycles. However, since the initial 0-cycle resistance of the small dies is inherently higher (approx. ~3.5mΩ), the relative 20% threshold provides a substantially wider tolerance window, placing the threshold at roughly 4.2 mΩ. This visual gap for small dies with high resistances can mask subtle degradation mechanisms. However, there are some notable outliers observed with high-Pb solders (see Figure 4b), which aligns with the large die observations of non-uniform degradation across the sample population. Conversely, a merely flat progression was observed for small dies with Ag-sinter material.

B. High Temperature Storage (HTS) Tests

As mentioned earlier, the high-temperature storage tests were performed only on samples with Ag-sinter material. Given that isothermal storage imposes significantly less thermomechanical stress than dynamic thermal cycling, the overall electrical degradation observed across all sample groups was minimal. Upon continuous exposure at 150°C for an extended duration of 2000 hours, the samples with large die (see figure 5a) and small die (see figure 5b) demonstrated relatively stable performance, with mean $R_{DS(on)}$ values well within the relative 20% threshold.

- For the large die samples (figure 5a), the measured $R_{DS(on)}$ remained stable throughout the testing period, reflecting highly uniform performance.

- For the small die samples (figure 5b), some outliers emerged, but remained below the threshold.

IV. Discussion

As discrete power semiconductors are transitioning toward wide-bandgap (WBG) devices, and regulatory exemptions for high-Pb solders face imminent phase-out, there is a growing need to demonstrate industrially compatible die-attach solutions. Pb-free alternatives must possess high electrical and thermal conductivity, resilience to thermomechanical loads, and the ability to be integrated into legacy production lines without major modifications.

The landscape of Ag-sinter materials ranges from pure Ag-sinter to resin-reinforced and hybrid pastes with additives. The application of these materials is largely dictated by die size and equipment capabilities. For instance, power modules typically rely on pressure-assisted pure Ag-sintering to yield high-density interconnects, regardless of die size. Conversely, discrete power semiconductors with smaller footprints often utilize pressureless Ag-sintering infused with resins within their porosity. While resin infused Ag-sinters are effective for smaller footprints, they frequently fail when scaled to larger die sizes (e.g., 25 mm^2). Recent developments focus on complex Ag-sinters with additives such as polymer spheres, which remain under evaluation due to lower and anisotropic conductivities, outgassing of high-temperature organics, and other processing challenges. Furthermore, most commercial Ag-sinters require specific substrate finishes, such as Ag or NiPdAu (PPF). Consequently, a pure Ag-sinter material that can be cured pressureless directly onto bare Cu substrates across a broad range of die sizes (2 mm^2 to 25 mm^2 in this study) has remained a critical area of interest. This study directly addressed this industry gap by evaluating pure Ag-sinter DA252 material that can be cured pressureless with processes that are compatible with current production lines.

From a processing perspective, the DA252 material exhib-

ited good dispensing behavior, minimal bondline shrinkage after curing, negligible void formation (<0.2%), and mechanically robust die attachment without requiring external pressure. In this study, the DA252 paste was dispensed immediately after acclimatization for two hours. However, upon subjecting the DA252 paste to centrifugal mixing at 500RPM for 50seconds, the dispensability of the paste was significantly improved. These observations indicate that the DA252 material can be integrated into conventional die-attach assembly lines with fewer modifications than pressure-assisted Ag-sintering technologies.

The lifetime reliability experiments further confirmed the benefits of the Ag-sintered interface. During thermal cycling, the differences between the die-attach technologies (solder vs sinter) were evident for the larger die configuration. The high-Pb solder exhibited a systematic increase in electrical on-state resistance $R_{DS(on)}$, whereas the DA252 samples maintained relatively stable $R_{DS(on)}$ over 2000 thermal cycles with fewer outliers exceeding the failure threshold. The probability distribution data also suggest that the degradation behavior of DA252 was more uniform across the sample population when compared to high-Pb solder reference samples. The dependence on die size further supports this interpretation. Smaller dies inherently experience lower thermomechanical strain due to their reduced footprint, allowing both solder and sinter materials to satisfy the AEC-Q101 qualification requirement. The high-temperature storage results provide complementary evidence. Since isothermal ageing introduces significantly lower mechanical stresses than thermal cycling, only minor changes in $R_{DS(on)}$ were observed over 2000 hours at $150°C$. Although this study demonstrates processability and reliability of DA252 material, there are some limitations to this study that need to be acknowledged.

1. In this study, the device health was primarily assessed through monitoring changes in $R_{DS(on)}$, providing an indirect indication of die-attach behavior. Complementary failure analysis, including Confocal Scanning Acoustic Microscopy (CSAM), cross-sectional analysis, and SEM inspection, would provide direct insight into the microstructural evolution of the DA252 paste and its dominant degradation mechanisms.
2. Besides, this study noted a distinct behavior. The die shear strength of DA252 material was observed to be higher at elevated temperatures than at room temperature. This distinct behavior requires further investigation in understanding the microstructural mechanisms driving this temperature-dependent strengthening behavior.

V. Conclusion

This study demonstrates that pressureless cured pure Ag-sintering materials, such as DA252, can be a potential Pb-free drop-in alternative for conventional high-Pb solders in cost-sensitive, high-volume discrete power semiconductor packaging. Although this work is one of several studies demonstrating the feasibility of pressureless Ag-sinter die-attach materials, the primary contribution of this work lies in defining and validating a practical framework of processability and reliability requirements for direct industrial integration. The DA252 material demonstrated relatively good processing, yielding a homogeneous die-attach interface with low voiding and high mechanical integrity, with stable electrical performance under accelerated thermal cycling and isothermal aging conditions. Future work will focus on addressing the limitations identified in this study, specifically conducting direct microstructural examinations to understand degradation mechanisms, and investigating the unique temperature-dependent shear strength behavior observed in the sintered joints.

Acknowledgment

The authors would like to express their sincere gratitude to the diverse academic community at the Chip Integration Technology Center (CITC) and Heraeus Materials Singapore, whose support, collaboration, and contributions made this work possible.

References

[1] N. P. Committee, "Sustained economic growth through technological progress," Nobel Prize in Economics documents 2025-2, Nobel Prize Committee, Oct 2025.

[2] A. Larsson, T. Tollefsen, O. Løvvik, and K. Aasmundtveit, "A review of eutectic au-ge solder joints," *Metallurgical and Materials Transactions A*, vol. 50, 07 2019.

[3] L. Jiang, R. Razak, B. Travis, G. Li, K. Zeng, R. Zhang, M. Khan, and R. Murugan, "Evaluation of au-si eutectic die-attach for power hermetic packages in space applications," *IMAPSource Proceedings*, vol. 2025, 11 2025.

[4] J. Xu, M. Wu, J. Pu, and S. Xue, "Novel au-based solder alloys: A potential answer for electrical packaging problem," *Advances in Materials Science and Engineering*, vol. 2020, no. 1, p. 4969647, 2020.

[5] F. Arabi, L. Theolier, D. Martineau, J.-Y. Deletage, M. Medina, and E. Woirgard, "Power electronic assemblies: Thermo-mechanical degradations of gold-tin solder for attaching devices," *Microelectronics Reliability*, vol. 64, pp. 409–414, 2016. Proceedings of the 27th European Symposium on Reliability of Electron Devices, Failure Physics and Analysis.

[6] A. Doroudi, A. Shamsipur, H. Omidvar, and M. Vatanara, "Effect of transient liquid phase bonding time on the microstructure, isothermal solidification completion and the mechanical properties during bonding of inconel 625 superalloy using cr-si-b-ni filler metal," *Journal of Manufacturing Processes*, vol. 38, pp. 235–243, 2019.

[7] K. H. K. N. Sohn Sunghyun, Kim Daewon, "Strategies to reduce transient liquid phase bonding time for the die attach of power semiconductors," *J Weld Join*, vol. 38, no. 2, pp. 158–165, 2020.

[8] C. Göbl and J. Faltenbacher, "Low temperature sinter technology die attachment for power electronic applications," in *2010 6th International Conference on Integrated Power Electronics Systems*, pp. 1–5, 2010.